

Facile preparation of η^6 -*p*-cymene ruthenium diphosphine complexes. Crystal structure of $[(\eta^6$ -*p*-cymene)Ru(dppf)Cl]PF₆

Svend B. Jensen, Susan J. Rodger, Mark D. Spicer *

Department of Pure and Applied Chemistry, University of Strathclyde, 295 Cathedral Street, Glasgow, G1 1XL, UK

Received 26 September 1997

Abstract

The clean, high yield synthesis of the complexes $[(\eta^6$ -*p*-cymene)Ru(P–P)Cl]PF₆ (P–P = diphosphine ligand) from $[(\eta^6$ -*p*-cymene)RuCl₂]₂ via $[(\eta^6$ -*p*-cymene)Ru(NCMe)₂Cl]PF₆ is reported for a series of ‘normal’ diphosphine ligands. The X-ray crystal structure of the 1,1'-bis(diphenylphosphino)ferrocene complex reveals the expected pianostool geometry, with the ligand cyclopentadienyl rings in the less usual eclipsed conformation. © 1998 Elsevier Science S.A. All rights reserved.

Keywords: Ruthenium; η^6 -arene; Diphosphine; Synthesis; X-ray structure

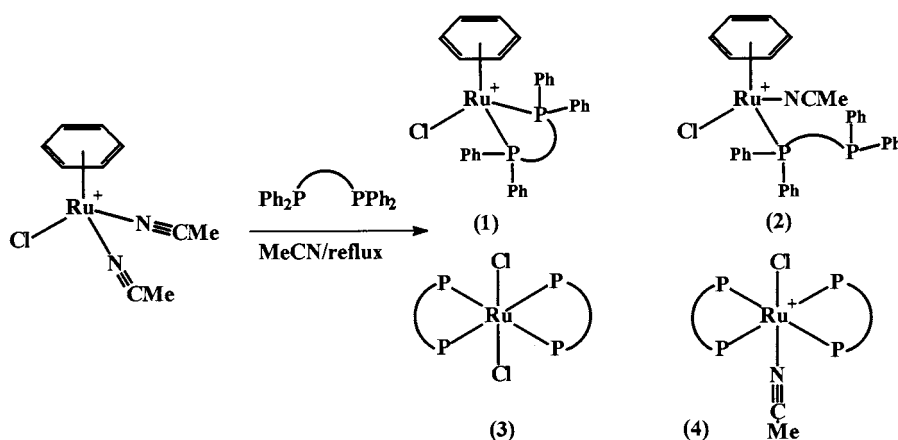
1. Introduction

The catalytic reactions of organoruthenium complexes have been extensively studied [1]. Recent work on η^6 -arene ruthenium systems has shown them to be active as catalysts for hydrogenation of olefins [2], ketones [3] and arenes [4]. In particular, η^6 -arene complexes with chiral phosphine auxiliaries have been found to be useful in asymmetric hydrogenation reactions [5,6]. Despite the utility of diphosphine derivatives, no truly convincing routes to such complexes have been forthcoming. A few examples of $[(\eta^6$ -arene)Ru(P–P)Cl]⁺ (P–P = diphosphine) complexes are known, but generally with unusually rigid ligands such as 1,2-bis(diphenylphosphino)benzene [7] or the chiral binaphthyl diphosphine, BINAP [5,6] and no viable route is reported from a single precursor. These complexes have also been obtained as unexpected products from reactions in arene solvents, for instance from the reaction of the 1,4-bis(diphenylphosphino)butane complex Ru₂Cl₄(dppb)₂(acetone)₂ with AgPF₆ in an acetone/toluene solvent system [8]. A recent paper has described the reactions of $[(\eta^6$ -C₆H₆)Ru(NCMe)₂Cl]PF₆

with a range of diphosphines and reports that in most cases a mixture of products is obtained [9]. These include the desired $[(\eta^6$ -C₆H₆)Ru(P–P)Cl]⁺ (**1**), $[(\eta^6$ -C₆H₆)Ru(NCMe)(κ -P–P)Cl]PF₆ (**2**) in which the phosphine is co-ordinated in a monodentate fashion, and under more forcing conditions, arene displacement occurs with the concomitant formation of *trans*-Ru(P–P)₂Cl₂ (**3**) and *trans*-[Ru(P–P)₂(NCMe)Cl]⁺ (**4**) (see Scheme 1). This is clearly not ideal. A number of alternative ruthenium complexes, $(\eta^6$ -C₆H₆)RuCl₂L (L = CH₃CN, PPh₃ or dmsO) were also tested as precursors, but with no success. The acetonitrile complex was too insoluble to be useful, the PPh₃ complex only reacts very slowly to yield complexes $[(\eta^6$ -C₆H₆)RuCl(PPh₃)(P–P)]⁺ where the diphosphine is co-ordinated in a monodentate fashion, while the dmsO complex gives a mixture of the desired product and $[(\eta^6$ -C₆H₆)RuCl₂]₂(μ -P–P) in which the diphosphine bridges the two ruthenium centres.

Our interest in these compounds arose from a desire to use the disubstituted phosphine complexes $[(\eta^6$ -C₆H₆)Ru{PhHP(CH₂)_nPHPh}Cl]⁺ (*n* = 2,3) for the template mediated functionalisation of the phosphine ligands. When the preparation of these complexes failed an investigation of the substitution reactions was un-

* Corresponding author. E-mail: m.d.spicer@strath.ac.uk



Scheme 1. Production of complexes 1–4 by arene displacement.

dertaken in an effort to understand this failure. We now report the results of this study, including the facile synthesis of pure $[\eta^6\text{-}(p\text{-cymene})\text{Ru}(\text{P}-\text{P})\text{Cl}]\text{PF}_6$ with a wide variety of diphosphines from the corresponding bis acetonitrile precursor, and the crystal structure of the 1,1'-bis(diphenylphosphino)ferrocene derivative.

2. Experimental

2.1. General

All NMR spectra were measured on a Bruker AMX400 spectrometer in CDCl_3 solutions. ^1H (400.16 MHz) and ^{13}C (100.13 MHz) spectra were referenced internally to the solvent peaks (and in turn to TMS), while ^{31}P spectra (161.98 MHz) were referenced to external 85% H_3PO_4 . Both ^{13}C and ^{31}P spectra were subject to broad band proton decoupling. FAB mass spectra were obtained on a JEOL JMS-AX505HA Mass spectrometer system using *m*-nitrobenzyl alcohol as matrix.

2.2. Reagents

The following were prepared by literature routes; $\text{Fe}(\eta^5\text{-C}_5\text{H}_4\text{PPh}_2)_2$ (dppf) [10], $\text{Ph}_2\text{PCH}_2\text{PPh}_2$ (dppm) [11], *cis*- $\text{Ph}_2\text{PCH}=\text{CHPPh}_2$, (vpp) [12], *o*- $\text{C}_6\text{H}_4(\text{PPh}_2)_2$ (pp) [13]. The following were obtained commercially and used as received; $\text{Ph}_2\text{P}(\text{CH}_2)_n\text{PPh}_2$ ($n = 2$ (dppe), 3 (dppp)) (Strem), α -terpinene (Aldrich). $\text{RuCl}_3 \cdot \text{H}_2\text{O}$ was a gift (Johnson Matthey). Solvents were used without purification and all reactions were performed under a N_2 atmosphere.

2.3. Preparation of $[(\eta^6\text{-}p\text{-cymene})\text{RuCl}_2]_2$ (5)

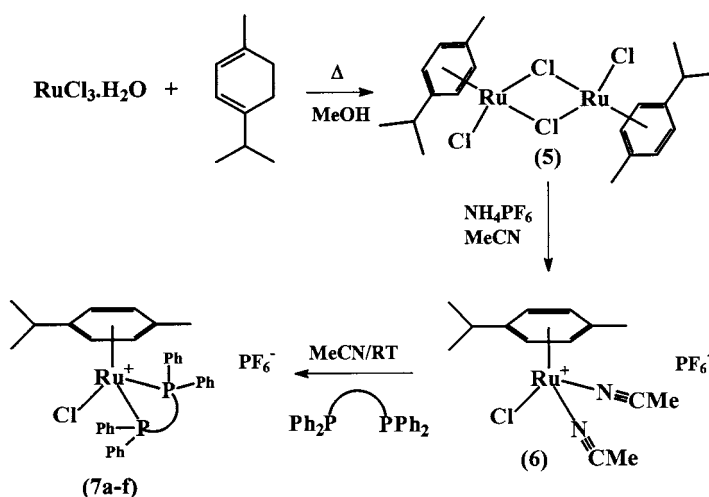
The method of Bennett et al. [14] was adapted as follows. $\text{RuCl}_3 \cdot \text{H}_2\text{O}$ (1.77 g, 8.5 mmol) and α -terpinene

(15 ml, 85%, technical grade) in absolute ethanol (100 ml) were refluxed for 4 h. On cooling, the product was deposited as a red-brown crystalline solid, was filtered, washed with ice cold methanol and dried in vacuo. Yield 1.60 g. A further crop of product was obtained by evaporating the burgundy filtrate to dryness, washing with diethyl ether to remove any excess α -terpinene and redissolving in methanol. After filtration the volume was reduced until precipitation began and the solution refrigerated. A further 0.25 g of product was obtained. Total yield, 1.85 g, 77%.

Analysis. Calc. for $\text{C}_{10}\text{H}_{14}\text{Cl}_2\text{Ru}$: C, 39.23; H, 4.61; Cl, 23.16%. Found: C, 39.10, H, 4.57, Cl, 23.13%. ^1H - and ^{13}C -NMR resonances were in agreement with literature values.

Table 1
Crystallographic data for (7a)

Formula	$\text{C}_{44}\text{H}_{42}\text{ClF}_6\text{FeP}_3\text{Ru}$
Formula weight	970.10
Unit cell	Monoclinic
Space group	$P2_1/n$ (# 14)
<i>a</i> , <i>b</i> , <i>c</i> (Å)	13.329(3), 14.975(2), 20.899(3)
β (°)	103.93(1)
<i>V</i> , Å ³	4048(1)
<i>F</i> (000)	1968.00
<i>D</i> _{calc.} , g cm ⁻³	1.591
μ (Mo-K α), cm ⁻¹	9.76
Measured reflections	7762
Unique reflections	7421 ($R_{\text{int}} = 0.088$)
No. observations ($F > 2\sigma(F)$)	3388
No. of refined parameters	505
<i>R</i>	0.055
<i>R</i> _w	0.062
Weighting scheme	$1/\sigma^2(F_o) = 4F_o^2/\sigma^2(F_e^2)$
Max shift/esd in final LS cycle	0.01
Residual electron density	-0.70–+0.74 eÅ ⁻³
GOF	1.70

**Ligands:**

Fe{ η^5 -C₅H₄(PPh₂)₂} (7a), Ph₂P(CH₂)_nPPh₂ (n=1 (7b), n=2 (7c), n=3 (7e))
cis-Ph₂PCH=CHPPh₂ (7d), o-C₆H₄(PPh₂)₂ (7f).

Scheme 2. Production of [(η^6 -p-cymene)Ru(diphosphine)Cl]PF₆ (7).

2.4. Preparation of [(η^6 -p-cymene)Ru(NCCH₃)₂Cl]PF₆ (6)

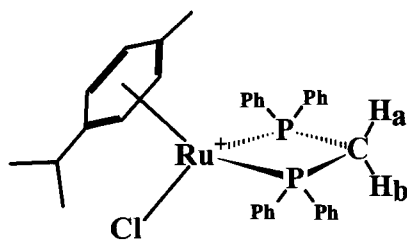
A suspension of (5) (1.9007 g, 3.1 mmol) and NH₄PF₆ (1.0611 g, 6.51 mmol) in acetonitrile (30 ml) was stirred overnight at room temperature (r.t.). This was filtered to remove NH₄Cl formed in the reaction and the orange filtrate taken to dryness to yield an orange oil. Extended trituration with diethyl ether followed by refrigeration (–18°C) resulted in a yellow-orange solid. This was filtered, washed with diethyl ether and dried in vacuo. Yield 2.87 g, 93%.

Analysis. Calc for C₁₄H₂₀ClF₆N₂PRu: C, 33.78; H, 4.05; N, 5.63; Cl, 7.12%. Found: C, 33.34; H, 3.78; N, 5.38; Cl, 7.07%. ¹H-NMR chemical shifts δ ppm: 1.30 (d, 6H, CH(CH₃)₂), 2.23 (s, 3H, C₆H₄CH₃), 2.60 (s, 6H, NCCH₃), 2.75 (sept, 1H, CH(CH₃)₂), 5.15 (d, 2H, η^6 -C₆H₄), 5.67 (d, 2H, η^6 -C₆H₄). ¹³C-NMR chemical shifts, δ ppm: 4.14 (NCCH₃), 19.03 (C₆H₄CH₃), 22.30 (CH(CH₃)₂), 31.60 (CH(CH₃)₂), {79.07, 85.52, 101.90, 108.99} (η^6 -C₆H₄), 128.23 (CN).

2.5. Preparation of [(η^6 -p-cymene)Ru(dppf)Cl]PF₆ (7a)

A solution of (6) (0.78 g, 1.57 mmol) and dppf (1.05 g, 1.89 mmol) in CHCl₃ (50 ml) was refluxed for 72 h. The solvent was evaporated to give a burgundy oil and CHCl₃ (10 ml) was added. The mixture was refrigerated overnight giving a brown solid. Washing with toluene followed by recrystallisation from hot methanol gave red crystals (1.28 g, 84%).

Analysis. Calc for C₄₄H₄₂ClF₆FeP₃Ru: C, 54.48; H, 4.36; Cl, 3.65; P, 9.58%. Found: C, 54.46; H, 4.43; Cl, 3.42; P, 10.08%. ¹H-NMR chemical shifts δ ppm: 0.89 (d, 6H CH(CH₃)₂), 0.98 (s, 3H, C₆H₄CH₃), 2.65 (sept, 1H, CH(CH₃)₂), 4.08 (s, 2H, Cp), 4.28 (s, 2H, Cp), 4.36 (s, 2H, Cp), 5.07 (s, 2H, Cp), 5.15 (br s, 2H, η^6 -C₆H₄), 5.70 (br s, 2H, η^6 -C₆H₄), 7.28–7.74 (m, 20H, Ph). ¹³C-NMR chemical shifts δ ppm: 17.80 (C₆H₄CH₃), 20.84 (CH(CH₃)₂), 31.22 (CH(CH₃)₂), {69.26, 73.86, 74.92, 78.75, 84.15 (virtual triplet)} (Cp), {90.94, 96.44, 99.43, 101.6} (η^6 -C₆H₄), {128.68, 130.26, 131.05, 132.47, 133.24, 135.33} (Ph). ³¹P-NMR chemical shifts, δ ppm: +37.1(s), –143.7 (sept).

Fig. 1. The [(η^6 -p-cymene)Ru(dppm)Cl]⁺ cation showing the inequivalence of the ligand backbone protons.

2.6. Preparation of [(η^6 -p-cymene)Ru(P–P)Cl]PF₆ (P–P = diphosphine), general procedure

A solution of (6) (0.129 g, 0.26 mmol) and the ligand (0.26 mmol) in acetonitrile (30 ml) was stirred for 16 h at r.t. The solvent was removed in vacuo, and the residue suspended in diethyl ether. After stirring for a few minutes the solid was filtered off, washed further with ether to remove any unreacted ligand and air dried.

Table 2
Ring contributions to ^{31}P NMR coordination shifts for $[(\eta^6\text{-}p\text{-cymene})\text{Ru}(\text{P}-\text{P})\text{Cl}]^+$ complexes

P–P	δ (^{31}P) complex	δ (^{31}P) ligand	Coordination shift ($\Delta\delta$) ^a	Ring contribution (Δ_r) ^b
$2 \times \text{PPh}_3$	+24.6	–5.9	+30.5	—
<i>o</i> - $\text{C}_6\text{H}_4(\text{PPh}_2)_2$	65.7	–2.2	+67.9	+37.4
$2 \times \text{PMePh}_2$	+21.7	–28.0	+49.7	—
$\text{Ph}_2\text{P}(\text{CH}_2)\text{PPh}_2$	+2.7	–22.6	+25.3	–24.4
$\text{Ph}_2\text{P}(\text{CH}_2)_2\text{PPh}_2$	+72.1	–13.3	+85.4	+35.7
$\text{Ph}_2\text{P}(\text{CH}_2)_3\text{PPh}_2$	+25.5	–17.3	+42.8	–6.9

^a δ (^{31}P) complex — δ (^{31}P) ligand.

^b $\Delta\delta$ (chelate) — $\Delta\delta$ (monodentate).

2.7. $[(\eta^6\text{-}p\text{-cymene})\text{Ru}\{\text{Ph}_2\text{PCH}_2\text{PPh}_2\}\text{Cl}]\text{PF}_6$ (**7b**)

An analytical sample was obtained by the slow evaporation of a toluene/dichloromethane solution. Analysis. Calc for $\text{C}_{35}\text{H}_{36}\text{ClF}_6\text{P}_3\text{Ru}\cdot\text{CH}_2\text{Cl}_2$: C, 48.86; H, 4.33; Cl, 12.02; P, 10.50%. Found: C, 49.12; H, 4.39; Cl, 11.62; P, 10.11%. ^1H -NMR chemical shifts δ ppm: 1.02 (d, 6H, $\text{CH}(\text{CH}_3)_2$), 1.42 (s, 3H, $\text{C}_6\text{H}_4\text{CH}_3$), 2.41 (sept, 1H, $\text{CH}(\text{CH}_3)_2$), 4.54 (d of t, 1H, $\text{P}-\text{CH}_2-\text{P}$), 4.95 (d of t, 1H, $\text{P}-\text{CH}_2-\text{P}$), 6.05 (d, 2H, $\eta^6\text{-C}_6\text{H}_4$), 6.17 (d, 2H, $\eta^6\text{-C}_6\text{H}_4$), 7.31–7.62 (m, 20H, Ph). ^{13}C -NMR chemical shifts δ ppm: 17.33 ($\text{C}_6\text{H}_4\text{CH}_3$), 21.98 ($\text{CH}(\text{CH}_3)_2$), 31.13 ($\text{CH}(\text{CH}_3)_2$), 41.85 (t, $^1J_{31\text{P}-13\text{C}} = 31$ Hz, $\text{P}-\text{CH}_2$), {90.32, 92.04, 102.10, 120.97} ($\eta^6\text{-C}_6\text{H}_4$), 128.8–133.0 (Ph). ^{31}P -NMR chemical shifts, δ ppm: +2.7(s), –143.3 (sept).

2.8. $[(\eta^6\text{-}p\text{-cymene})\text{Ru}\{\text{Ph}_2\text{P}(\text{CH}_2)_2\text{PPh}_2\}\text{Cl}]\text{PF}_6$ (**7c**)

An analytical sample was obtained by low temperature crystallisation from chloroform. Analysis. Calc. for $\text{C}_{36}\text{H}_{38}\text{ClF}_6\text{P}_3\text{Ru}\cdot 0.5\text{CHCl}_3$: C, 50.16; H, 4.44; Cl, 10.14; P, 10.63%. Found: C, 50.67; H, 4.50; Cl, 10.25; P, 10.25%. ^1H -NMR chemical shifts, δ ppm: 0.80 (d, 6H, $\text{CH}(\text{CH}_3)_2$), 1.11 (s, 3H, $\text{C}_6\text{H}_4\text{CH}_3$), 2.29 (sept, 1H, $\text{CH}(\text{CH}_3)_2$), 2.53 (m, 2H, $\text{P}-\text{CH}_2$), 2.95 (m, 2H, $\text{P}-\text{CH}_2$), 5.88 (d, 2H, $\eta^6\text{-C}_6\text{H}_4$), 5.98 (d, 2H, $\eta^6\text{-C}_6\text{H}_4$), 7.24–7.73 (m, 20H, Ph). ^{13}C -NMR chemical shifts, δ ppm: 15.77 ($\text{C}_6\text{H}_4\text{CH}_3$), 21.18 ($\text{CH}(\text{CH}_3)_2$), 26.31 (t, $^1J_{31\text{P}-13\text{C}} = 22$ Hz, $\text{P}-\text{CH}_2$), 30.81 ($\text{CH}(\text{CH}_3)_2$), {92.15, 94.47, 100.78, 123.83} ($\eta^6\text{-C}_6\text{H}_4$), 128.8–134.5 (Ph). ^{31}P -NMR chemical shifts, δ ppm: +72.1 (s), –143.5 (sept).

2.9. $[(\eta^6\text{-}p\text{-cymene})\text{Ru}\{\text{cis-Ph}_2\text{PCH}=\text{CHPPh}_2\}\text{Cl}]\text{PF}_6$ (**7d**)

Analysis. Calc. for $\text{C}_{36}\text{H}_{36}\text{ClF}_6\text{P}_3\text{Ru}$: C, 53.24; H, 4.47; Cl, 4.37; P, 11.44%. Found: C, 53.09; H, 4.59; Cl, 4.25; P, 10.75%. ^1H -NMR chemical shifts, δ ppm: 0.92 (d, 6H, $\text{CH}(\text{CH}_3)_2$), 1.05 (s, 3H, $\text{C}_6\text{H}_4\text{CH}_3$), 2.20 (sept, 1H, $\text{CH}(\text{CH}_3)_2$), 5.91 (d, 2H, $\eta^6\text{-C}_6\text{H}_4$), 6.19 (d, 2H, $\eta^6\text{-C}_6\text{H}_4$), 7.65 (d, 2H, $\text{P}-\text{CH}$), 7.24–7.74 (m, 20H, Ph). ^{31}P -NMR chemical shifts, δ ppm: +75.7 (s), –143.5 (sept).

2.10. $[(\eta^6\text{-}p\text{-cymene})\text{Ru}\{\text{Ph}_2\text{P}(\text{CH}_2)_3\text{PPh}_2\}\text{Cl}]\text{PF}_6$ (**7e**)

Analysis. Calc. for $\text{C}_{37}\text{H}_{40}\text{ClF}_6\text{P}_3\text{Ru}$: C, 53.66; H, 4.87; Cl, 4.28; P, 11.22%. Found: C, 53.27; H, 4.72; Cl, 4.23; P, 10.88%. ^1H -NMR chemical shifts, δ ppm: 0.83 (d, 6H, $\text{CH}(\text{CH}_3)_2$), 1.38 (s, 3H, $\text{C}_6\text{H}_4\text{CH}_3$), 2.26 (m, 5H, $\text{CH}(\text{CH}_3)_2$ and PCH_2), 3.02 (m, 2H, $\text{CH}_2\text{CH}_2\text{CH}_2$), 5.67 (d, 2H, $\eta^6\text{-C}_6\text{H}_4$), 5.79 (d, 2H, $\eta^6\text{-C}_6\text{H}_4$), 7.28–7.74 (m, 20H, Ph). ^{13}C -NMR chemical shifts δ ppm: 16.66 ($\text{C}_6\text{H}_4\text{CH}_3$), 20.43 ($\text{CH}(\text{CH}_3)_2$), 21.36 (PCH_2CH_2), 24.39 (virtual triplet, $J = 18$ Hz, $\text{P}-\text{CH}_2$), 30.63 ($\text{CH}(\text{CH}_3)_2$), {93.46, 94.38, 102.54, 124.88} ($\eta^6\text{-C}_6\text{H}_4$), 128.6–136.7 (Ph). ^{31}P -NMR chemical shifts, δ ppm: +25.5(s), –143.5 (sept).

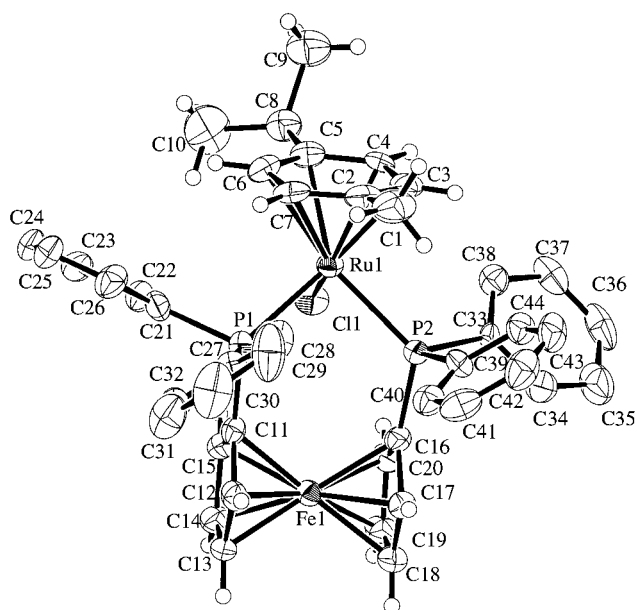


Fig. 2. ORTEP diagram of the cation of (**7a**) with the thermal ellipsoids at the 40% level and showing the atom numbering scheme. The ligand phenyl protons are omitted for clarity.

Table 3
Non-hydrogen positional parameters and isotropic temperature factors (B_{eq}) for (**7a**)

Atom	x	y	z	B_{eq}
Ru(1)	0.02825(06)	0.75514(06)	0.42139(04)	2.66(3)
Fe(1)	0.30466(11)	0.57687(09)	0.45396(07)	2.83(6)
Cl(1)	0.0400(02)	0.63897(18)	0.50094(13)	3.8(1)
P(1)	0.2059(02)	0.78751(17)	0.46804(13)	2.7(1)
P(2)	0.0650(02)	0.64016(17)	0.35379(13)	2.6(1)
P(3)	0.9450(03)	0.1641(03)	0.17983(19)	5.2(2)
F(1)	0.9954(08)	0.1872(09)	0.2508(05)	13.8(7)
F(2)	0.8642(09)	0.2329(09)	0.1864(06)	16.7(8)
F(3)	0.8825(12)	0.0947(09)	0.2014(07)	18(1)
F(4)	1.0186(09)	0.0905(09)	0.1712(07)	17(1)
F(5)	1.0152(17)	0.2281(11)	0.1623(08)	25(2)
F(6)	0.8903(11)	0.1452(08)	0.1072(04)	15.5(8)
C(1)	-0.0320(10)	0.8992(09)	0.2827(06)	5.9(7)
C(2)	-0.0469(09)	0.8622(08)	0.3468(05)	4.0(5)
C(3)	-0.1163(08)	0.7911(08)	0.3466(05)	3.8(5)
C(4)	-0.1478(07)	0.7664(07)	0.4041(05)	3.3(4)
C(5)	-0.1034(08)	0.8111(07)	0.4637(06)	3.6(5)
C(6)	-0.0328(09)	0.8761(07)	0.4671(05)	3.9(5)
C(7)	-0.0017(08)	0.9000(07)	0.4083(06)	3.9(5)
C(8)	-0.1467(09)	0.7816(07)	0.5236(06)	4.5(5)
C(9)	-0.2621(10)	0.8124(10)	0.5109(07)	6.7(8)
C(10)	-0.0863(12)	0.8174(14)	0.5883(07)	0(1)
C(11)	0.3019(08)	0.7004(06)	0.4928(04)	2.7(4)
C(12)	0.3942(08)	0.6891(06)	0.4693(05)	3.2(4)
C(13)	0.4484(08)	0.6162(07)	0.5033(05)	3.6(5)
C(14)	0.3944(08)	0.5819(07)	0.5478(05)	3.7(5)
C(15)	0.3027(08)	0.6334(07)	0.5422(05)	3.5(4)
C(16)	0.1743(07)	0.5663(06)	0.3816(05)	2.9(4)
C(17)	0.2644(08)	0.5524(07)	0.3555(05)	3.2(4)
C(18)	0.3199(08)	0.4795(07)	0.3880(06)	4.1(5)
C(19)	0.2672(09)	0.4463(07)	0.4341(06)	4.4(5)
C(20)	0.1785(08)	0.4973(06)	0.4293(05)	3.6(5)
C(21)	0.2160(08)	0.8480(07)	0.5453(05)	3.4(5)
C(22)	0.1921(08)	0.8035(07)	0.5992(05)	3.7(5)
C(23)	0.1973(09)	0.8462(09)	0.6583(06)	4.6(6)
C(24)	0.2253(10)	0.9354(09)	0.6652(06)	5.0(6)
C(25)	0.2466(09)	0.9814(08)	0.6124(06)	4.8(6)
C(26)	0.2410(09)	0.9377(07)	0.5536(06)	4.4(5)
C(27)	0.2725(08)	0.8629(06)	0.4226(05)	2.9(4)
C(28)	0.2251(10)	0.8926(07)	0.3609(06)	4.6(6)
C(29)	0.2726(14)	0.9524(10)	0.3278(07)	7.6(8)
C(30)	0.3703(15)	0.9829(10)	0.3563(07)	7.3(8)
C(31)	0.4195(11)	0.9522(09)	0.4163(07)	6.2(7)
C(32)	0.3728(08)	0.8921(07)	0.4514(05)	3.9(5)
C(33)	-0.0330(08)	0.5523(06)	0.3317(05)	2.9(4)
C(34)	-0.0127(09)	0.4843(07)	0.2919(06)	4.4(5)
C(35)	-0.0752(11)	0.4110(08)	0.2759(07)	6.5(7)
C(36)	-0.1637(11)	0.4079(09)	0.2995(07)	5.6(6)
C(37)	-0.1870(09)	0.4747(09)	0.3376(06)	4.7(6)
C(38)	-0.1205(08)	0.5468(07)	0.3557(05)	3.6(5)
C(39)	0.0761(08)	0.6799(07)	0.2732(05)	3.5(5)
C(40)	0.1648(09)	0.7216(07)	0.2652(06)	3.8(5)
C(41)	0.1701(10)	0.7558(09)	0.2041(06)	5.1(6)
C(42)	0.0841(11)	0.7517(09)	0.1520(06)	5.4(6)
C(43)	-0.0031(10)	0.7125(08)	0.1591(05)	4.7(6)
C(44)	-0.0075(08)	0.6778(07)	0.2194(05)	3.6(5)

2.11. $[(\eta^6\text{-}p\text{-cymene})\text{Ru}\{\text{o-C}_6\text{H}_4(\text{PPh}_2)_2\}\text{Cl}]\text{PF}_6$ (**7f**)

An analytical sample was obtained by the slow evap-

Table 4
Selected bond lengths (Å) and angles (°) of (**7a**)

Bond lengths			
Ru(1)–Cl(1)	2.385(3)	Fe(1)–C(19)	2.04(1)
Ru(1)–P(1)	2.384(3)	Fe(1)–C(20)	2.02(1)
Ru(1)–P(2)	2.352(3)	P(1)–C(11)	1.81(1)
Ru(1)–C(2)	2.29(1)	P(1)–C(21)	1.83(1)
Ru(1)–C(3)	2.23(1)	P(1)–C(27)	1.835(9)
Ru(1)–C(4)	2.293(9)	P(2)–C(16)	1.81(1)
Ru(1)–C(5)	2.30(1)	P(2)–C(33)	1.83(1)
Ru(1)–C(6)	2.29(1)	P(2)–C(39)	1.83(1)
Ru(1)–C(7)	2.21(1)	C(1)–C(2)	1.51(1)
Fe(1)–C(11)	2.024(9)	C(2)–C(3)	1.41(1)
Fe(1)–C(12)	2.041(9)	C(2)–C(7)	1.40(1)
Fe(1)–C(13)	2.03(1)	C(3)–C(4)	1.41(1)
Fe(1)–C(14)	2.04(1)	C(4)–C(5)	1.41(1)
Fe(1)–C(15)	2.04(1)	C(5)–C(6)	1.34(1)
Fe(1)–C(16)	2.02(1)	C(5)–C(8)	1.56(1)
Fe(1)–C(17)	2.03(1)	C(6)–C(7)	1.43(1)
Fe(1)–C(18)	2.05(1)	C(8)–C(9)	1.57(2)
		C(8)–C(10)	1.50(2)
Bond angles			
Cl(1)–Ru(1)–P(1)	88.35(9)	Cl(1)–Ru(1)–P(2)	84.06(10)
P(1)–Ru(1)–P(2)	93.70(9)	P(2)–Ru(1)–C(2)	102.9(3)
P(2)–Ru(1)–C(3)	91.5(3)	P(1)–Ru(1)–C(6)	95.0(3)
P(1)–Ru(1)–C(7)	89.0(3)	Cl(1)–Ru(1)–C(4)	93.2(3)
		Cl(1)–Ru(1)–C(5)	85.7(3)
Ru(1)–P(1)–C(11)	122.2(3)	Ru(1)–P(2)–C(16)	121.5(3)
Ru(1)–P(1)–C(27)	118.0(3)	Ru(1)–P(2)–C(33)	116.0(3)
Ru(1)–P(1)–C(21)	108.5(3)	Ru(1)–P(2)–C(39)	113.0(3)
C(11)–P(1)–C(21)	102.0(4)	C(16)–P(2)–C(33)	96.4(4)
C(11)–P(1)–C(27)	101.2(4)	C(16)–P(2)–C(39)	104.9(5)
C(21)–P(1)–C(27)	102.1(5)	C(33)–P(2)–C(39)	102.3(5)

oration of a toluene/dichloromethane solution. Analysis. Calc. for $\text{C}_{40}\text{H}_{38}\text{ClF}_6\text{P}_3\text{Ru}\cdot\text{C}_6\text{H}_7$: C, 59.15; H, 4.86; Cl, 3.72; P 9.74%. Found: C, 59.33, H, 4.78; Cl, 3.60; P, 9.81%. $^1\text{H-NMR}$ chemical shifts, δ ppm: 0.81 (d, 6H, $\text{CH}(\text{CH}_3)_2$), 1.50 (s, 3H, $\text{C}_6\text{H}_4\text{CH}_3$), 2.44 (sept, 1H, $\text{CH}(\text{CH}_3)_2$), 5.98 (br s, 4H, $\eta^6\text{-C}_6\text{H}_4$), {7.02 (m, 4H), 7.30 (t, 4H), 7.44 m (2H), 7.53 (m, 6H), 7.57 (d, 2H), 7.70 (m, 2H), 7.87 (m, 4H)} $\{\eta^6\text{-C}_6\text{H}_4\}$ (*o*- $\text{C}_6\text{H}_4/\text{Ph}$). $^{13}\text{C-NMR}$ chemical shifts, δ ppm: 17.13 ($\text{C}_6\text{H}_4\text{CH}_3$), 21.27 ($\text{CH}(\text{CH}_3)_2$), 31.37 ($\text{CH}(\text{CH}_3)_2$), {92.51, 94.77, 102.47, 124.83} ($\eta^6\text{-C}_6\text{H}_4$), 128.8–141.1 (*o*- $\text{C}_6\text{H}_4/\text{Ph}$). $^{31}\text{P-NMR}$ chemical shifts, δ ppm: +65.7 (s), –143.6 (sept).

2.12. X-ray Crystal structure of (**7a**)

Red prismatic crystals of (**7a**) were obtained by dissolving a crude sample in hot methanol and allowing to cool slowly. A crystal of suitable quality and dimensions was mounted on a glass fibre for data collection. Details of the X-ray data collection and refinement are summarised in Table 1. The heavy atom positions were located by Patterson methods [15] and the remaining non-hydrogen atom positions were found using Fourier techniques [16]. The PF_6^- ion was found to be some-

Table 5
Comparison of the ruthenium coordination spheres for $[(\eta^6\text{-arene})\text{Ru}(\text{P},\text{P})\text{Cl}]^+$ ions

Complex	d(Ru–Cl) Å	d(Ru–P) Å	$\angle \text{P–Ru–P}$ (°)	$\angle \text{P–Ru–Cl}$ (°)	d(Ru–C) Å Range (average)	d(Ru–C ₆ H ₆) ^a Å	Reference
$[(p\text{-cy})\text{Ru}(\text{dppf})\text{Cl}]^+$	2.387(3)	2.353(3) 2.381(3)	93.6(1)	84.1(1) 88.3(1)	2.210(1)–2.300(1) (2.27)	1.784(9)	This work
$[(\text{tol})\text{Ru}(\text{dppb})\text{Cl}]^+$	2.399(2)	2.332(2) 2.349(2)	92.30(6)	86.30(7) 89.35(7)	2.200–2.333 (2.256)	1.772(3)	[8]
$[(\text{C}_6\text{H}_6)\text{Ru}(\text{binap})\text{Cl}]^+$	2.393(4)	2.334(3) 2.379(3)	91.4(1)	84.9(1) 89.1(1)	2.255–2.302 (2.273)	1.770	[6]
$[(\text{tol})\text{Ru}(\text{PPh}_3)_2\text{Cl}]^+$	2.389(3)	2.384(3) 2.399(3)	100.3(1)	85.3(1) 89.3(1)	2.214–2.347 (2.285)	1.780	[20]

^a d(Ru–C₆H₆) = Ru to arene centroid distance.

what disordered and no attempt to model this was entirely satisfactory. An absorption correction (DI-FABS [17]) was applied to an isotropic model. Subsequently, all non-H atoms were refined anisotropically. Many of the hydrogen atoms were located in the difference maps, but H-atoms were inserted at calculated positions, with temperature factors $B_{\text{H}} = 1.25B_{\text{C}}$.

3. Results and discussion

The starting material for this chemistry, the *p*-cymene ruthenium dichloride dimer (**5**) has been previously prepared from ruthenium chloride and α -phellandrene [14]. During the course of our studies we discovered that substitution with technical grade α -terpinene also gave the desired product with no diminution of the yield obtained. The crystalline dimer is obtained in ca 80% yield by refluxing $\text{RuCl}_3 \cdot \text{H}_2\text{O}$ and α -terpinene in ethanol. This is converted in turn to $[\eta^6\text{-}(p\text{-cy})\text{Ru}(\text{NCMe})_2\text{Cl}]\text{PF}_6$ (**6**) by the method of McCormick et al. [7], stirring with one equivalent of NH_4PF_6 in acetonitrile solution. The product is somewhat resistant to crystallisation, but after removal of solvent in vacuo and trituration with ether for several days a yellow-orange powder is obtained which analyses satisfactorily and has $\nu(\text{C}\equiv\text{N}) = 2301(\text{w})$ and

2329(m) cm^{-1} . This is an excellent precursor for the formation of the diphosphine complexes. Reaction of (**6**) with one equivalent of diphosphine in acetonitrile solution at r.t. yields the desired $[(\eta^6\text{-}p\text{-cymene})\text{Ru}(\text{diphosphine})\text{Cl}]\text{PF}_6$ species (**7**) (Scheme 2). NMR of the reaction mixture shows the reactions to go essentially to completion. However the isolated yields are in the range 50–70% due to the high solubility of these complexes and their propensity to form intractable oils. No other products have been observed to form in these reactions, in stark contrast to the reactions of the analogous η^6 -benzene derivatives. In that case, reaction at r.t. resulted primarily in the formation of (**2**), while attempts to drive the reaction to completion by refluxing resulted in arene displacement to give products (**3**) and (**4**), as previously observed. The less forcing reaction conditions (r.t.) required in this system are apparently a reflection of the greater lability of the MeCN ligands in the *p*-cymene complex and are clearly not sufficiently severe to induce displacement of the co-ordinated arene group.

The diphosphine complexes (**7a–f**) are obtained as air stable yellow-orange microcrystalline solids, whose spectroscopic and analytical data is entirely in keeping with their structures. The ¹H-NMR spectra show resonances characteristic of η^6 -*p*-cymene and the diphosphine ligand in question. In the cases of dppm and dppf the symmetry of the ligand environment is lowered on complexation to the metal. In the former this is manifest by the non equivalence of the $-\text{PCH}_2\text{P}-$ protons each of which appears as a multiplet, while in the latter the ferrocenyl ring protons appear as four multiplets as opposed to the two seen in the free ligand. In both cases this is induced by the asymmetry of the co-ordination environment, as illustrated for (**7b**) in Fig. 1. The ³¹P-NMR spectra show a septet due to the free PF_6^- ion and a singlet from the coordinated phosphine. Co-ordination shifts typical of chelated diphosphine complexes are observed in keeping with the ring contri-

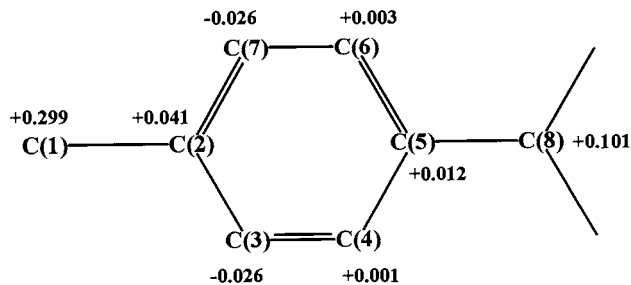


Fig. 3. Deviations from the least squares plane of the η^6 -*p*-cymene group in (**7a**).

Table 6
Comparison of structural parameters for dppf ligands coordinated to ruthenium

Complex	d(Ru–P) Å	∠P–Ru–P (°)	Tilt ^a (°)	d(Ru...Fe) Å	d(P...P) Å	Reference
[Ru(dppf)(CO)HCl(PPh ₃)	2.518(4) ^b 2.392(4) ^c	102.2(0)	3.01	4.30	3.82	[25]
[(η^5 -C ₅ H ₅)Ru(dppf)H] ^d	2.263(4) 2.246(3) 2.265(3) 2.258(3)	99.1(1) 95.5(1)	4.85 6.27	4.34 4.33	3.43 3.35	[22]
[(η^5 -C ₅ Me ₅)Ru(dppf)H]	2.271(1) 2.259(1)	97.9(1)	7.21	4.38	3.42	[23]
(7a)	2.353(3) 2.381(3)	93.6(1)	1.82	4.47	3.46	This work

^a Dihedral angle between cyclopentadienyl ring least squares planes.

^b P *trans* to H.

^c P *trans* to P.

^d Two unique molecules in the asymmetric unit.

bution formalism proposed by Garrou [18]. Thus, the ring contributions (Δ_r) to the coordination shifts may be calculated in the cases where suitably analogous monodentate phosphine complexes are available. We have previously prepared [$(\eta^6$ -*p*-cymene)Ru(PR₃)₂Cl]⁺ (PR₃=PPh₃, PMePh₂) (M.D. Spicer, R.R. Rowlings, unpublished results) and the shifts on coordination for these monodentate phosphines may be compared with the coordination shifts of Ph₂P(CH₂)_{*n*}PPh₂ (*n* = 1–3) (PMePh₂), and *o*-C₆H₄(PPh₂)₂ (PPh₃). The data are tabulated in Table 2 and show that with respect to the non-chelated analogues the 4-membered ring (Δ_r = –24.4 ppm) is shielded more than the 6-membered ring (Δ_r = –6.9 ppm) while the 5-membered rings are deshielded (Δ_r = +35.7 (Ph₂P(CH₂)₂PPh₂) and +37.4 ppm (*o*-C₆H₄(PPh₂)₂)). FAB Mass spectra have been obtained for each of the complexes, which confirm the compositions of the molecular ions, [$(\eta^6$ -*p*-cymene)Ru(P–P)Cl]⁺, and show fragmentation consistent with initial chloride loss, followed by loss of the *p*-cymene. In the case of the dppf complex there is also evidence for a second fragmentation pathway in which *p*-cymene is lost prior to halide. In general, the complexity of the isotope patterns, with many overlapping peaks, has precluded the measurement of high precision molecular masses.

3.1. X-ray Crystal Structure of [$(\eta^6$ -*p*-cymene)Ru(dppf)Cl]PF₆ (7a)

An ORTEP diagram of the cation and its labelling scheme are shown in Fig. 2. Atomic positional parameters are given in Table 3, selected bond lengths and angles in Table 4 and a comparison of structural parameters pertaining to the coordination sphere for (7a), [$(\eta^6$ -C₆H₆)Ru(BINAP)Cl]⁺, [$(\eta^6$ -C₆H₅CH₃)Ru(dppb)Cl]⁺, and [$(\eta^6$ -C₆H₅CH₃)Ru(PPh₃)₂Cl]⁺ in

Table 5. The cation may be thought of as having a *fac*-octahedral coordination sphere, with three sites occupied by the η^6 -*p*-cymene ligand and the remaining three by the two phosphorus and one chlorine donor atoms. The Ru(1)–P(1), Ru(1)–P(2) and Ru(1)–C(1) bond lengths are comparable with other examples of such derivatives (see Table 5), while the bond angles deviate a little from the 90° expected for a pure octahedral complex, for instance the bond angle P(1)–Ru–P(2) at 93.70(9)° is greater than the idealised angle. It can be seen that the nature of the phosphine does have some influence on the geometry at the metal which is probably best rationalised in terms of ligand flexibility, which in turn allows the accommodation of the sterically demanding phenyl groups. For instance, 1,4-bis(diphenylphosphino)butane, dppb, while potentially having the greater bite size in reality gives a relatively small angle at the Ru centre. This probably arises from its greater conformational mobility which allows it to accommodate a bond angle close to 90° despite its longer backbone. The large P–Ru–P angle in the PPh₃ complex (100.3°) is a reflection of the relative steric demands of the two bulky phosphine ligands when compared to a single bidentate ligand. The distance of the *p*-cymene ring centroid from the ruthenium centre is 1.784 Å, very similar to the distance in the related complexes (Table 5). The ring itself deviates from planarity. The displacements from the least-squares plane are shown in Fig. 3, and suggest a slight ‘fold’ along an axis running through C(3) and C(7), and this is also supported by inspection of the Ru–C bond distances. Both alkyl substituents are markedly displaced from the plane (CH₃, 0.299; ^{*i*}Pr, 0.101 Å) which presumably is a result of the steric requirements of the ligand phenyl groups. The dppf ligand conformation can be compared with that in other structurally characterised dppf-ruthenium complexes. There are four, namely

$[(\eta^5\text{-C}_5\text{H}_5)\text{Ru}(\text{dppf})\text{H}]$ [21], $[(\eta^5\text{-C}_5\text{Me}_5)\text{Ru}(\text{dppf})\text{H}]$ [22], $[(\eta^5\text{-C}_5\text{Me}_5)\text{Ru}(\text{dppf})(\eta^2\text{-O}_2)]\text{BF}_4$ [23] and $[\text{Ru}(\text{CO})\text{ClH}(\text{PPh}_3)(\text{dppf})]$ [24]. The relevant structural parameters are shown in Table 6 [25]. In each case the ligand cyclopentadienyl rings are essentially planar with dihedral angles between the planes (ring tilt) in the approximate range $1.8\text{--}7.2^\circ$, with the current structure being at the lower end of the range. The Fe–Ru separation is typically about $4.3\text{--}4.5 \text{ \AA}$. The major structural difference in the present complex is that the dppf cyclopentadienyl rings are eclipsed, while in each of the other examples they are staggered. The effect of this is to induce a twist of the ferrocenyl moiety. This is illustrated in Fig. 4 where (7a) and $[(\eta^5\text{-C}_5\text{Me}_5)\text{Ru}(\text{dppf})\text{H}]$ are compared. In the present complex Fe(1), C(11), C(16) (the ipso cyclopentadienyl carbons) P(1) and P(2) are approximately coplanar (mean deviation from least squares plane = 0.0265 \AA). In the other complexes, while the Fe and two P atoms remain

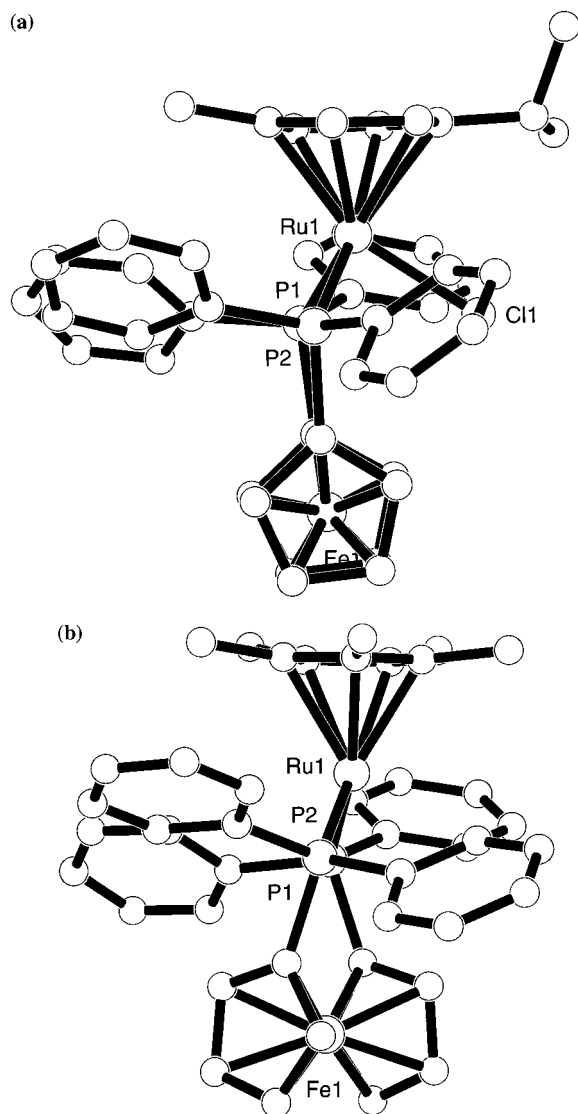


Fig. 4. Structures of (a) (7a) and (b) $[(\eta^5\text{-C}_5\text{Me}_5)\text{Ru}(\text{dppf})\text{H}]$ highlighting the differences in conformation of the dppf ligands.

co-planar, the ipso carbons are disposed one above and one below the plane resulting in a substantial overall twist of the ferrocenyl group.

Acknowledgements

We wish to thank Strathclyde University (SBJ) the EPSRC (SJR) and the Nuffield Foundation (MDS) for funding and Johnson Matthey PLC for the generous loan of ruthenium trichloride. We also wish to acknowledge the use of the EPSRC's Chemical Database Service at Daresbury.

References

- [1] M.A. Bennett, T.W. Matheson, in: G. Wilkinson, F.G.A. Stone, E.W. Abel (Eds.), *Comprehensive Organometallic Chemistry*, Pergamon Oxford, 1982, p. 931.
- [2] M.A. Bennett, J.P. Ennett, *Inorg. Chim. Acta* 198–200 (1992) 583.
- [3] M. Kitamura, M. Tokunaga, T. Ohkuma, R. Noyori, *Tetrahedron Letts.* 32 (1991) 4163.
- [4] M.A. Bennett, T.-N. Huang, A.K. Smith, T.W. Turney, *J. Chem. Soc. Chem. Commun.* (1978) 582.
- [5] K. Mashima, K. Kusano, T. Ohta, R. Noyori, H. Takaya, *J. Chem. Soc. Chem. Commun.* (1989) 1208.
- [6] K. Mashima, K. Kusano, N. Sato, Y. Matsumura, K. Nozaki, H. Kumobayashi, Y. Hori, T. Ishizaki, S. Akutagawa, H. Takaya, *J. Org. Chem.* 59 (1994) 3064.
- [7] F.B. McCormick, D.D. Cox, W.B. Gleason, *Organometallics* 12 (1993) 610.
- [8] I.S. Thorburn, S.J. Rettig, B.R. James, *J. Organometal. Chem.* 296 (1985) 103.
- [9] D.E. Fogg, B.R. James, *J. Organometal. Chem.* 462 (1993) C21.
- [10] J.J. Bishop, A. Davidson, M.L. Katcher, D.W. Lichtenberg, R.E. Merrill, J.C. Smart, *J. Organometal. Chem.* 27 (1971) 241.
- [11] A.M. Aguiar, J. Beisler, *J. Org. Chem.* 29 (1964) 1660.
- [12] A.M. Aguiar, D. Daigle, *J. Am. Chem. Soc.* 86 (1964) 2299.
- [13] S.J. Higgins, Ph.D. Thesis, University of Southampton, 1984.
- [14] M.A. Bennett, T.-N. Huang, T.W. Matheson, A.K. Smith, *Inorg. Synth.* 21 (1982) 74.
- [15] P.T. Beurskens, G. Admiraal, G. Beurskens, W.P. Bosman, S. Garcia-Granda, R.O. Gould, J.M.M. Smits, C. Smykalla, PATTY, The DIRDIF programme system, Technical Report of the Crystallography Laboratory, University of Nijmegen, The Netherlands.
- [16] TeXsan, Crystal Structure Analysis Package, Molecular Structure Corporation, Woodlands, TX, 1985, 1992.
- [17] N. Walker, D. Stuart, *DIFABS*, *Acta Crystallogr.* A39 (1983) 158.
- [18] (a) S.O. Grim, W.L. Briggs, R.C. Barth, C.A. Tolman, J.P. Jesson, *Inorg. Chem.* 13 (1974) 1095. (b) P.E. Garrou, *Chem. Rev.* 81 (1981) 229.
- [20] J.R. Polam, L.C. Porter, *Inorg. Chim. Acta* 205 (1993) 119.
- [21] M.I. Bruce, I.R. Butler, W.R. Cullen, G.A. Koutsantonis, M.R. Snow, E.R.T. Tiekink, *Aust. J. Chem.* 41 (1988) 963.
- [22] R.T. Hembre, J.S. McQueen, V.W. Day, *J. Am. Chem. Soc.* 118 (1996) 798.
- [23] M. Sato, M. Asai, *J. Organomet. Chem.* 508 (1996) 121.
- [24] A. Santos, J. Lopez, J. Montoya, P. Noheda, A. Romero, A.M. Echavarren, *Organometallics* 13 (1994) 3605.
- [25] F.H. Allen, J.E. Davies, J.J. Galloy, O. Johnson, O. Kennard, C.F. Macrae, E.M. Mitchell, G.F. Mitchell, J.M. Smith, D.G. Watson, *J. Chem. Inf. Comp. Sci.* 31 (1991) 187.